YOLOv5-OLCAM-Based Target Detection and RRT-PRM Path Planning for Soccer Robots under Uncertain Conditions

Xinglei Chen[1], Feng Liu[2*]
[1]School of Education, Longdong University, Qingyang, 745000, China
[2]Physical Education Research Department, Xinjiang University, Urumqi, 830046, China
E-mail: chenxl792025ldxy@126.com, liufengaass@163.com
[*]Corresponding author

Keywords: RRT algorithm, football robots, target recognition, control strategy, path planning

Received: March 31, 2025

Robots still face enormous challenges in soccer matches, as the environment is complex and ever-changing. Robots need to perceive the positions and trajectories of teammates, opponents, and the ball in real time. Therefore, based on the You Only Look Once v5 model, an improved object recognition method is designed using a lightweight convolutional attention module. A path planning method is constructed by combining the rapidly-exploring random tree algorithm with the Probabilistic Roadmap method. Finally, a soccer robot control strategy incorporating the rapidly-exploring random tree algorithm is proposed. The research used a ball detection dataset J, specifically designed for the Robot Soccer Standard Platform League for testing. The research results showed that the accuracy and running time of the improved target recognition algorithm under size images were 99.12% and 0.19ms, respectively. The path planning algorithm, integrating the rapidly-exploring random tree algorithm, also performed well, requiring only 800 iterations to obtain the shortest planned path, which was 19.637cm. Compared with other mainstream methods, the improved method had significant advantages in path length and iteration times ($p<0.001$), indicating its practicality and robustness under uncertain conditions. In the comparison of control strategies, the research method had the lowest global decision entropy of 0.934 and the shortest average planning time of 26.8 seconds. The research method can significantly improve the intelligence level of soccer robots in competitions and assist soccer robots in making optimal control decisions on the field, achieving more efficient collaboration.

Povzetek: Razvit je YOLOv5-OLCAM za prepoznavo ter RRT-PRM z Bézierjem za planiranje poti in Petri-krmiljenje; doseže krajše in bolj gladke poti ter hitrejše odločitve.

1 Introduction

The sports field has always been an important part of human activities, and technological advancements have made robot athletes a hot topic in the sports field. Especially in high-demand sports such as soccer, robot athletes have shown their strong potential and future prospects [1]. On the one hand, as a representative of high-tech integration, Soccer-robots (SRs) require high standards in terms of motion performance, reaction speed, coordination, and accuracy [2-4]. Soccer matches involve fast decision-making, complex dynamic balance control, and precise motion trajectories, which require very high technical requirements for robots [5]. On the other hand, SR also provides a very feasible and attractive application scenario for the promotion of Artificial Intelligence (AI) technology [6]. In the future, soccer may become an important project in robotics competition, and the goal of RoboCup is to develop a robot that can defeat the human world champion team by 2050 [7].

X. Chen et al. proposed a path planning method based on an adaptive Genetic Algorithm (GA) according to the characteristics of SR. This method solved the obstacle avoidance problem of SR planning paths in a short period, and its path planning ability was significantly better than traditional GA [8]. Y. Zhang et al. analyzed the stability, working parameters, and division of labor and cooperation between STM32 and 51 series microcontrollers of the SR system through theoretical analysis and experimental verification, and determined the final control method. This method could accurately complete the kicking action and identify the soccer and goal, which can meet the expected design requirements [9]. A. F. V. Muzio et al. focused on learning SR behavior, which involves completing the task of dribbling on the track and against individual opponents as much as possible. This method used a hierarchical controller for operation, where model-free learning strategy and a model-based walking algorithm interacted. In the simulation experiment, this method outperformed the manual coding behavior used by the ITAndroids robot team in 68.2% of dribbling attempts [10]. X. Gan et al. proposed a novel dynamic parameter A* algorithm to address the problem of unmanned ground vehicles lacking self-optimization and learning capabilities in spaces containing a large number of unknown obstacles. In terms of convergence speed, memory system consumption, and optimization ability of path planning, this method outperformed Q-learning and A* algorithm [11]. A. Zou et al. designed a fusion improved mayfly optimization

algorithm based on Q-learning and the dynamic window method to address

Table 1: Summary of related work.

Method	Performance	Experimental environment	Limitation
X. Chen et al.'s Path Planning Method Based on Adaptive GA	Path planning capability superior to traditional GA, solving short-term obstacle avoidance problems	Static environment, fixed obstacles	Poor adaptability to dynamic environments, high path redundancy, and high computational complexity
Y. STM32 and 51 microcontroller control by Zhang et al	Complete the kicking action, identify the soccer and goal	Simple experimental scenarios, fixed tasks	Insufficient adaptability to complex dynamic scenes and poor real-time performance
A. F. V. Muzio et al.'s Learning Behavior Method Based on Hierarchical Controllers	68.2% of dribbling attempts are better than manual coding	Simulation experiment, single opponent scenario	Dependent on simulation environment, the dynamic collaboration ability in actual competitions has not been verified
X. Gan et al.'s dynamic parameter A * algorithm	Fast convergence speed, low memory consumption, and superior path planning optimization ability compared to Q-learning and A*	Unknown obstacle space	Good performance in static environments, but insufficient real-time performance in dynamic environments
A. Zou et al.'s Improved Dragonfly Optimization Algorithm Based on Q-learning and Dynamic Window Method Fusion	Addressing the stability and convergence speed issues of path planning in static environments	100×100 static map, 20 random experiments	Poor adaptability to dynamic environments and insufficient path smoothness
G. Hu et al.'s enhanced slime mold algorithm based on Bezier curve	Short path length and high smoothness	Smooth Path Planning for Mobile Robots	High computational complexity and poor real-time performance
M. Steve et al.'s Regulatory Pure Tracking Algorithm	High security, quick assessment	Observable space	Low efficiency in path planning and limited adaptability to dynamic environments

poor stability, slow convergence velocity, and limited applicability to static environments in robot path planning utilizing basic mayfly optimization algorithms. This study conducted 20 random simulation experiments in a 100*100 static map environment, confirming the effectiveness of the research method in solving accuracy and speed [12]. G. Hu et al. put forth an enhanced slime mold algorithm based on Bezier curves to solve the smooth path planning issue of mobile robots, which is used to solve the smooth path planning model. Compared with other classical algorithms, this method had advantages in generating feasible paths with shorter length and higher smoothness [13]. M. Steve et al. designed a tuning pure pursuit algorithm that achieves progressive improvement over recent technologies by adjusting the linear velocity of the robot, particularly in terms of safety in observable space, and validated its fast evaluation [14]. By summarizing the relevant work content, Table 1 can be obtained.

In summary, current research achievements mainly focus on the control of SR and path planning of robots, but there are still problems such as insufficient obstacle avoidance ability, poor adaptability to dynamic environments, and weak robustness of target recognition and localization in complex environments. There are three main research questions. The first is how to improve the accuracy and efficiency of SR robot's target recognition in complex and dynamic soccer game environments. The second is how to design an efficient path planning method under uncertain conditions to ensure that the SR robot can smoothly and safely reach the task position. The third is how to construct a control strategy to improve the decision-making ability and overall performance of SR robots in actual competitions. The expected measurable results are as follows: firstly, through comparative experiments with existing advanced methods, the accuracy and runtime of target recognition under different image sizes are explored; Secondly, comparisons are made with other mainstream path planning methods on various experimental graphs, and evaluations are conducted using planned path length and visualized path trajectories; Thirdly, different control strategies are compared to evaluate the uncertainty and efficiency in the decision-making process. Therefore, the research is based on the You Only Look Once version5 (YOLO v5) and optimizes the YOLO v5 object recognition algorithm by adding a Lightweight Convolutional Attention Module (LCAM), resulting in a YOLO v5 Optimized Based on LCAM algorithm (YOLO v5-OLCAM). Then, the Rapidly-exploring Random Tree (RRT) algorithm is used for path planning, and the Probabilistic Roadmap Method (PRM) and Bezier curve are introduced for optimization, resulting in an improved RRT-PRM method. Finally, an SR control strategy incorporating the RRT algorithm is proposed. The research objective is to design a control strategy that can ensure SR can quickly and accurately identify targets in dynamic environments under uncertain conditions, and plan collision-free, smooth, and efficient paths in a short period, providing real-time optimal decisions. The innovation mainly includes the following three points. The first is to propose a YOLO v5-OLCAM algorithm for SR target recognition, which maintains low parameters and computational complexity while avoiding negative impacts on training and inference efficiency. The second is to design an improved path planning method for the RRT-PRM algorithm. It not only solves the redundancy problem of the RRT algorithm but also improves the efficiency and adaptability of path planning,

and it is more suitable for the dynamic motion requirements of robots under uncertain conditions. The third is to use a joint Petri net model to construct an SR

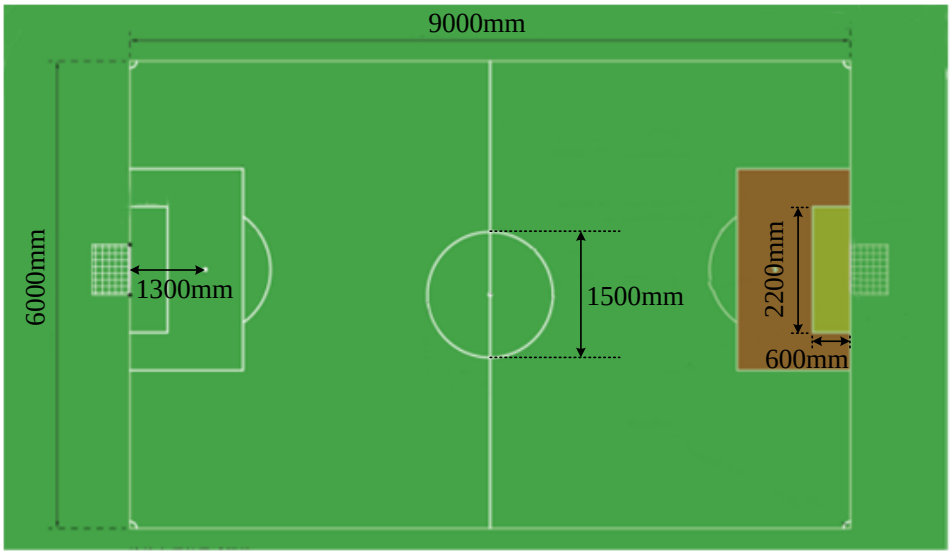

Figure 1: Schematic diagram of soccer match scene on RoboCup standard platform.

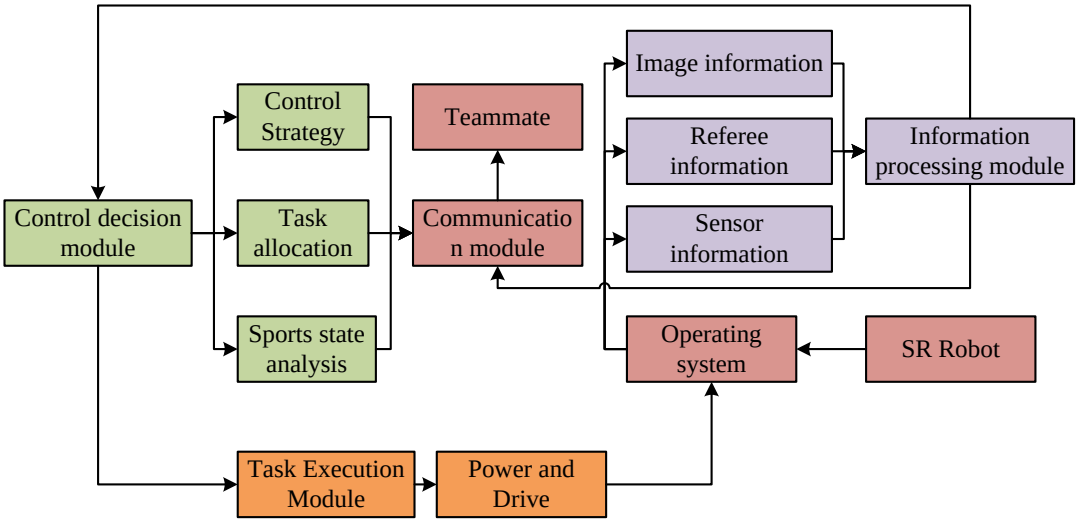

Figure 2: Schematic diagram of the model architecture of the experimental robot.

control strategy that integrates the RRT algorithm, achieving efficient task allocation and decision-making. The contribution lies in providing reliable foundational support for complex soccer game scenarios, reducing uncertainty and risks when making a decision, and improving the overall performance of SR during the game.

2 Methods and materials

To achieve precise target recognition and control of SR under uncertain conditions, this study first conducts motion analysis on SR and then designs a YOLO v5-OLCAM algorithm and an improved RRT-PRM algorithm for target recognition and path planning. Finally, a Petri-based control strategy is proposed.

2.1 Kinematic analysis for SR

Soccer, as a team sport, encourages collaboration and teamwork among players. By training and playing with teammates, players can rely on each other, divide their work, and work together to achieve common goals [15-17]. Therefore, soccer is not only a competitive sport but also a global phenomenon with profound social, cultural, and economic impacts. However, the current soccer game scene is complex, and target recognition needs to be completed quickly and accurately in a dynamic environment. At the same time, SR requires making decisions and actions in a short period, which places high demands on target recognition and control strategies and real-time performance [18-20]. Therefore, this study first constructs an SR-oriented model to lay a solid foundation for subsequent target recognition, path planning, and

control strategy tasks. The NAO robot has 25 degrees of freedom and can achieve flexible limb movements, including walking, running, passing, shooting, and saving [21]. Moreover, real-time data sharing can be achieved between robots through user datagram communication protocols, including information such as the position of the ball, teammates, and opponents. This

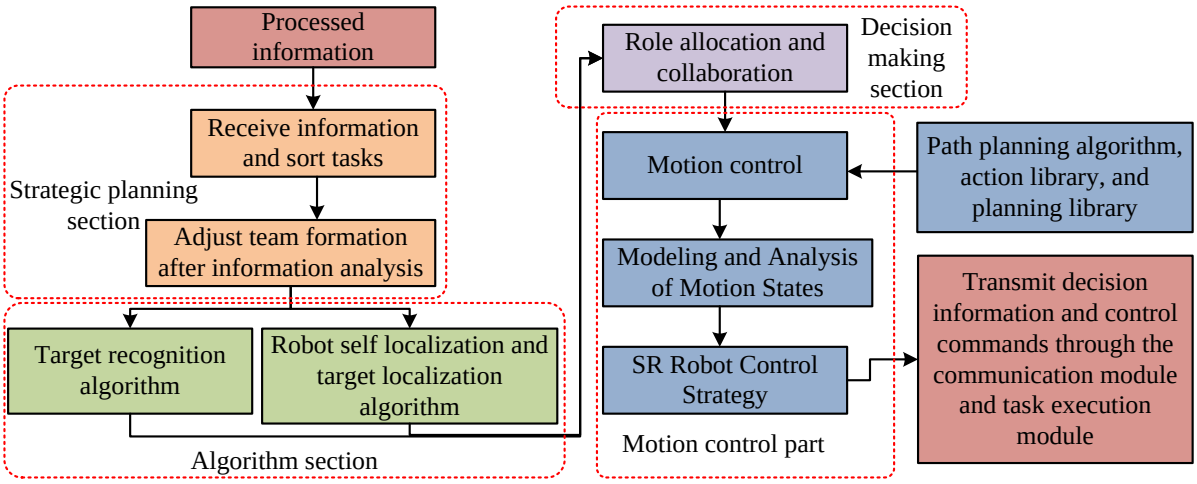

Figure 3: Process diagram of control decision module.

enables robots to better collaborate as a team, such as passing, defending, and attacking coordination [22-23]. In addition, as the designated robot for the RoboCup Standard Platform League, it provides a unified hardware platform for participating teams. This makes the competition fairer, and participating teams can focus on algorithm and strategy optimization. Therefore, this study chooses it as the experimental subject. Thesoccer match scene on the RoboCup standard platform is shown in Figure 1.

In Figure 1, as the difficulty of the field changes, the lighting conditions also change, and it is required that the light in a large area of the field is less than 300lx, and the ratio of the brightest and darkest lighting should not exceed 10:1. SR can process information centrally during soccer matches, and then provide corresponding strategies through the control system. Finally, the robot completes the execution of actions and transmits the information of collaborative work to teammates. The model architecture of the experimental robot is shown in Figure 2.

In Figure 2, the architecture is mainly divided into the information processing module, communication module, control decision module, and task execution module. Through the mutual cooperation between various modules, the collaborative tasks between robots in the competition can be achieved. The most important part is the control decision module, which is the key to achieving autonomous action. It can adjust the execution of actions in real-time through environmental information obtained from sensors, and dynamically adjust the execution strategy to ensure efficient completion of tasks. The specific process of this module is shown in Figure 3.

Figure 3 mainly includes the strategy planning part, the algorithm part, the decision-making part, and the motion control part. The first step is to receive and analyze the surrounding environmental information, then sort the next actions, and finally adjust the strategy based on the priority and difficulty of all tasks. In the motion control of SR, it is required to solve the forward and inverse kinematics. The forward kinematics analysis requires modeling the six-degree-of-freedom joints of the robot using the D-H method, and the mathematical expression is shown in equation (1).

$$A_j^{j-1}=\begin{bmatrix}\cos\theta_j & -\sin\theta_j\cos\vartheta_j & \sin\theta_j\sin\vartheta_j & l_j\cos\theta_j\\ \sin\theta_j & \cos\theta_j\cos\vartheta_j & -\cos\theta_j\sin\vartheta_j & l_j\sin\theta_j\\ 0 & \sin\vartheta_j & \cos\vartheta_j & d_j\\ 0 & 0 & 0 & 1\end{bmatrix} \quad (1)$$

In equation (1), A_j^{j-1} is the inverse matrix, which is a homogeneous transformation matrix. l_j, ϑ_j, d_j, and θ_j are the length, torsion angle, offset, and rotation angle of the j-th connecting rod or joint. Then, according to the chain rule, the homogeneous transformation matrix corresponding to the coordinate system transformation can be obtained, and combined with the D-H parameters, the end positions of each part of the SR can be obtained. In inverse kinematics analysis, this study solves the problem through analytical methods, and the required joint angles can be obtained by simply using the geometric relationships of the robot. Due to the symmetry of SR's body, this study selects the left leg for modeling, as shown in Figure 4.

In Figure 4, θ_{pitch} and θ_{roll} correspond to the pitch and roll angles of the ankle joint. θ_{knee} is the knee joint angle. Given the state of the hip and ankle joints, and representing the thigh and calf lengths of SR as L_{thigh} and L_{calf}, the vector g of the hip joint and the distance d_{h-a} from the hip to the ankle joint can be obtained, as calculated in equation (2).

$$\begin{cases} g=\left[g_x,g_y,g_z\right]^T \\ d_{h-a}=\sqrt{g_x^2+g_y^2+g_z^2}\end{cases} \quad (2)$$

In equation (2), g_x, g_y, and g_z are the components of the vector on the X, Y, and Z axes. The shape formed by three joints conforms to the triangle law, and θ_{knee} can be obtained as shown in equation (3).

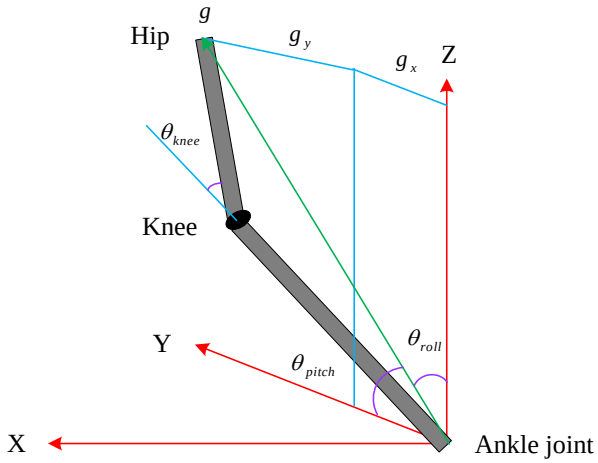

Figure 4: Schematic diagram of SR left leg inverse kinematics analysis.

$$\theta_{knee} = \pi - ar\cos\left[\left(L_{thigh}^2 + L_{calf}^2 - d_{h-a}^2\right)/\left(2L_{thigh}L_{calf}\right)\right] \quad (3)$$

Finally, by using the coordinate system of the ankle joint, θ_{pitch} and θ_{roll} can be obtained, as shown in equation (4).

$$\begin{cases} \theta_{pitch} = -\vartheta - \arctan\left[g_x \Big/ \left(S\left(g_z\right)\sqrt{g_y^2 + g_z^2}\right)\right] \\ \theta_{roll} = \arctan\left(g_y / g_z\right) \end{cases} \quad (4)$$

In equation (4), S is the sign function. Based on the above content, the kinematic analysis of SR can be completed.

2.2 Target recognition method based on improved YOLOv5

After the completion of the SR kinematic analysis and design, optimization can be carried out for its target recognition part. Among them, SR often requires a large amount of computing resources and memory for target recognition, and is sensitive to environmental factors such as lighting conditions and object occlusion. Therefore, this study uses convolutional neural networks as the basis, which perform very well in visual tasks, and introduces LCAM to improve the YOLO v5, resulting in the YOLO v5-OLCAM method. Firstly, in the YOLO v5 algorithm, it is mainly segmented into three parts: input, backbone network, output, and loss function [24-26]. The Complete Intersection over Union (CIoU) loss function introduces a correction factor to make the loss more robust to target boxes of different shapes. Therefore, it is used for processing, as expressed in equation (5) [27].

$$LOSS_{CIoU} = 1 - IoU + \frac{d^2(C_p, C_t)}{l_c^2} + \omega\zeta \quad (5)$$

In equation (5), IoU, ω, and ζ represent the consistency loss of intersection to union ratio, weight coefficient, and aspect ratio. $d^2(C_p, C_t)$ is the Euclidean distance between the center points of the predicted and true boxes, C_p and C_t. l_c is the diagonal length of the smallest closure box covering C_p and C_t. Generally, the classification loss is processed through a binary cross entropy function, as given by equation (6).

$$LOSS_{BCE} = -\frac{1}{N}\sum_{i-1}^{N}\left[y_i \log(\hat{y}_i) + (1 - y_i)\log(1 - \hat{y}_i)\right] \quad (6)$$

In equation (6), N and y are the total number of samples and the true label, and $\hat{y}$ is the probability that the predicted sample is a positive class. To improve the YOLOv5 object detection algorithm, the study is conducted to enhance the feature extraction capability through the LCAM module. Compared with other Convolutional Block Attention Modules and SENet attention mechanisms, this method is designed with fewer parameters and computational complexity, making it more suitable for real-time operation on resource-constrained robot platforms. It mainly consists of channel attention modules and spatial attention modules, which are beneficial for enhancing important features in feature maps and target recognition in complex and dynamic environments. The channel attention module is mainly responsible for the important features in the feature map. It compresses the spatial dimension of the feature map into a single value through global average pooling and global maximum pooling, then performs feature transformation through shared multi-layer perceptrons, and finally generates attention channel maps through the Sigmoid function [28-29]. The spatial attention module focuses on which pixels are important in the feature map. It first processes the output of the channel attention module to generate two two-dimensional feature maps, then concatenates the two feature maps and performs feature transformation through a convolutional layer, finally generating a spatial attention map [30-31].By element-wise multiplying the input features with the two attention maps mentioned above, the final output features can be obtained. This module has relatively small parameters and computational complexity, does not increase the training and inference overhead of the method, and can be integrated into any network architecture. Among them, the channel attention model includes one global average

pooling layer, one global maximum pooling layer, a shared multi-layer perceptron, and one Sigmoid function. The spatial attention module

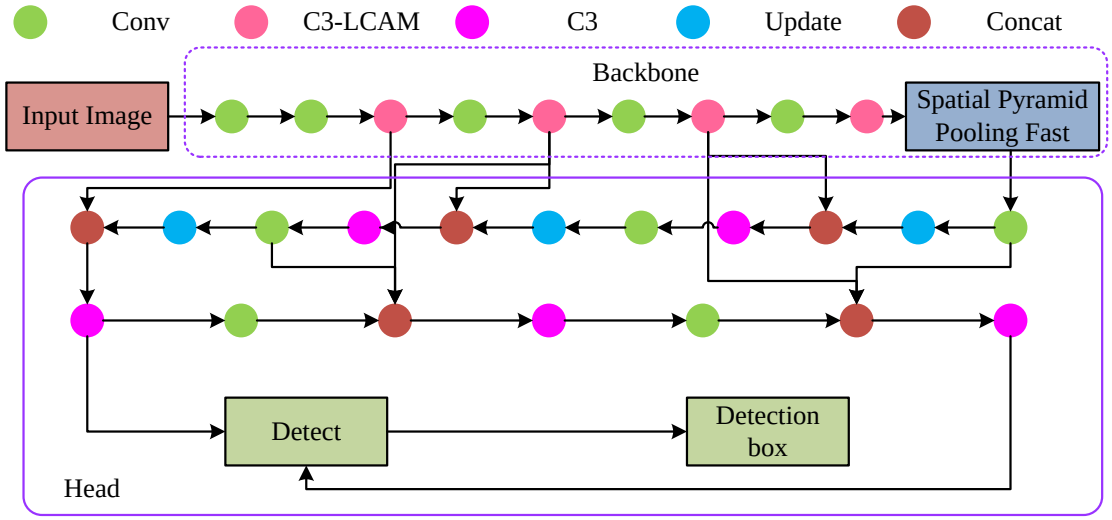

(a) YOLO v5 OLCAM Method Structure Diagram

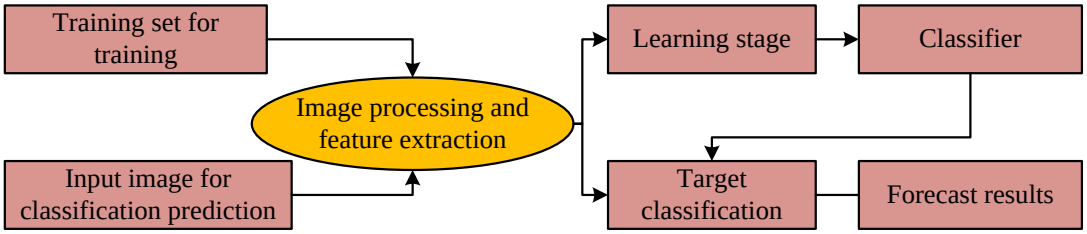

(b) YOLO v5 OLCAM Method Training Flowchart

Figure 5: Structure diagram and training flowchart of YOLO v5-OLCAM method.

includes channel convolution concatenation, 7*7 convolutional layers, and a Sigmoid function. The layer type for feature fusion and output is element-wise multiplication. In addition, this study optimizes the fusion of multi-scale feature networks. On the basis of the path aggregation network and feature pyramid network, it first removes nodes that are only used as inputs to simplify the network architecture, and then establishes a network layer with bidirectional paths. Finally, the weights corresponding to the features are configured through weighted summation. The fused output feature calculation is shown in equation (7).

$$T_{OC} = \sum_i \left[\left(I_i \square \omega'_i \right) \Big/ \tau \sum_j \omega'_j \right] \tag{7}$$

In equation (7), I_i and ω'_i correspond to the i-th input feature and its weight parameters. τ is a very small constant. In summary, the structure diagram and training process of YOLOv5-OLCAM method can be obtained, as shown in Figure 5.

In Figure 5, during the training process of YOLOv5-OLCAM, the first step is to construct a dataset containing the target object. Then, the input image is preprocessed to meet the input size requirements of the method. Next, convolutional layers are utilized to extract image features, and the obtained features are processed to predict the category and position of the target object, and finally, output the prediction result. The LCAM module is located in the Head section of the YOLOv5 model, which enhances the feature map by introducing attention mechanisms to improve the model's ability to recognize targets.

2.3 Path planning method integrating RRT algorithm under uncertain conditions

After the design of the target recognition method in SR is completed, to achieve the designated position in the planning decision, it is generally reflected through a motion control function. However, this approach relies on feedback from sensors, and its control response speed is limited, making it unsuitable for more complex tasks. Therefore, this study introduces the RRT algorithm for path planning. This algorithm has advantages such as fast exploration, high computational efficiency, and proficiency in parallelization processing. The most important thing is that it does not rely on prior knowledge of the environment and can adapt to uncertain conditions or dynamically changing environments. However, the RRT algorithm may suffer from path redundancy in path planning. Therefore, this study integrates the PRM method and combines it with an improved Bezier curve to obtain

an improved RRT-PRM path planning method. In the RRT section, it generates a random extended tree by selecting an initial point as the root node and adding leaf nodes through random sampling. When the leaf nodes contain the target point or

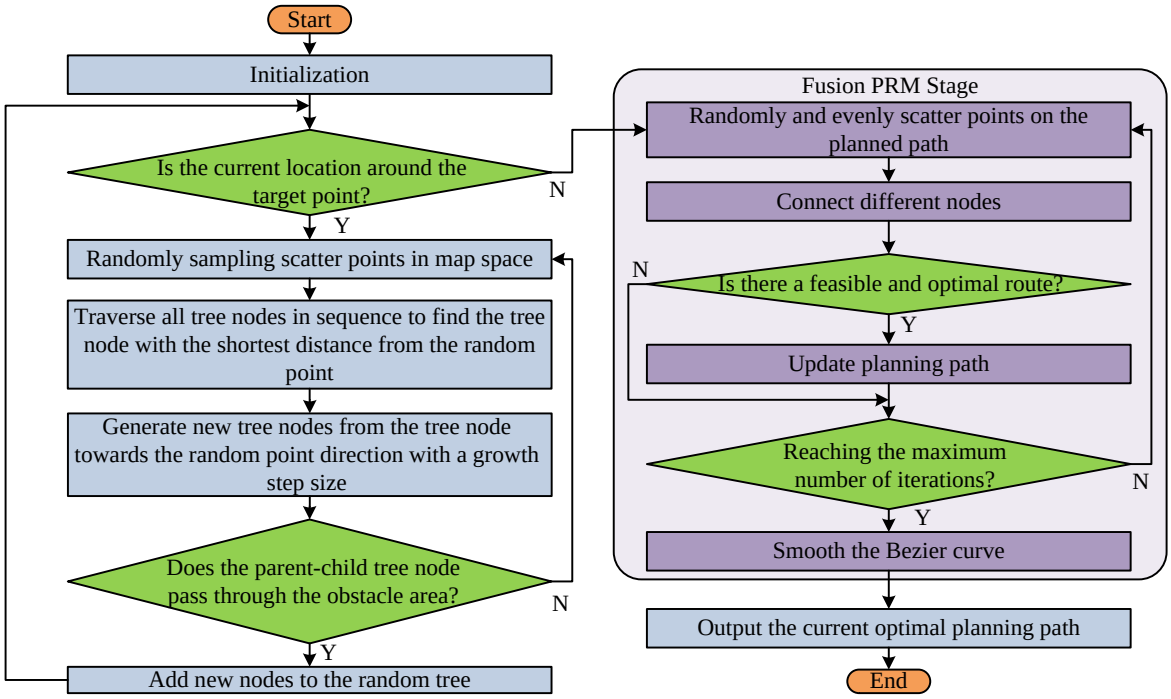

Figure 6: Flow chart of path planning method for integrating RRT algorithm under uncertain conditions.

enter the target area, the path from the initial to the target points can be searched through backtracking in the random tree species. The PRM method includes a learning phase and a query phase. The former requires more time, while the latter only requires inputting relevant information. Then, by combining the roadmap information obtained during the learning phase, a collision-free route from the initial position to the target position can be searched for in a relatively short period. In the fusion process of PRM, the first step is to randomly and uniformly place the nodes into the path planned by the RRT algorithm. Then, the nodes are connected, and collision detection is completed. If no collision occurs, it will be included in the path and further judged whether it is a shorter path: if so, an update will be made; otherwise, the above operation will continue to loop until the termination condition is reached, and the best path can be output. However, the best path obtained from this is the polyline obtained through nodes, which cannot meet the motion law of SR. System oscillation can be caused without considering path curvature, which has a negative impact on the stability of SR. The Bezier curve can make the path planning smoother and simplify the motion route with a small number of key points, as calculated in equation (8).

$$P(c)=\sum_{i=0}^{n} B_i^n(c)\cdot P_i \tag{8}$$

In equation (8), P_i is the coordinate of the i -th control point. c , n , and $B_i^n(c)$ are the parameters, order, and Bernstein basis functions of 0-1. The smoothing process for this study selects a third-order Bezier curve for calculation, as shown in equation (9).

$$P'(c)=(1-c)^3\cdot P_0+3c(1-c)^2\cdot P_1+3c^2(1-c)\cdot P_2+c^3\cdot P_3 \tag{9}$$

In equation (9), P_0 to P_3 are continuous control nodes on the planned path to be fitted. Given this, the flowchart of the path planning method that integrates RRT algorithm under uncertain conditions is shown in Figure 6.

In Figure 6, the integration of improved PRM and RRT is mainly divided into three stages. The first stage is the RRT fast exploration stage, which randomly samples and generates a tree path based on the current position of the robot as the root node. The second stage is PRM path optimization, which uniformly inserts PRM random nodes on the initial path generated by RRT. The third stage is Bézier curve smoothing to improve the efficiency and safety of robot motion.

2.4 Design of SR control strategy integrating RRT algorithm

After the design of the target recognition method and path planning method for SR mentioned above, to assist SR in making appropriate control decisions under uncertain conditions, the first step is to focus on different state behaviors during the motion process. This study uses an object-oriented approach to complete character modeling and analyzes the motion state of SR through Petri nets. In the process of character modeling, there are mainly four types of roles: left forward and midfield forward, left back and right back, and goalkeeper. In the Petri net processing,

the expression for workflow net $\sum$ is first set to equation (10).

$$\begin{cases} \sum = (IN, S_T, S', OUT) \\ S' = \{S'_0, ..., S'_{end}\}, IN, OUT : S' \square S_T \rightarrow S' \end{cases} \quad (10)$$

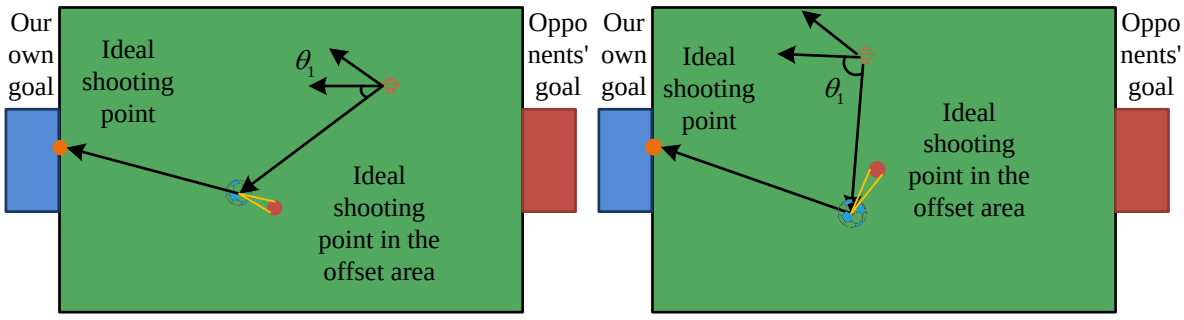

(a) Positive perspective (b) Lateral perspective

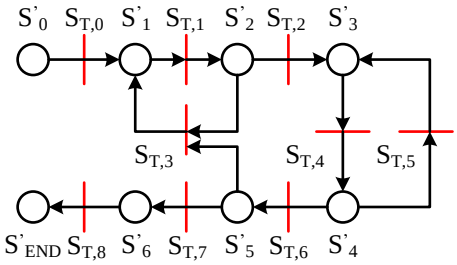

(c) Petri net modeling diagram

Figure 7: Petri net modeling diagram and SR kicking display diagram at different orientations.

In equation (10), IN, S_T, S', and OUT are input functions, state transition conditions, current position, and output functions. S'_{end} is the position at the end. The calculation of the forward's workflow network is shown in equation (11).

$$\sum = \begin{cases} \{S'_0, ..., S'_6, S'_{END}\} \\ \{S_{T,0}, ..., S_{T,8}\} \\ IN(S_{T,0}) = S'_0, OUT(S_{T,0}) = S'_1; ...; IN(S_{T,2}) = S'_2, OUT(S_{T,2}) = S'_3 \\ IN(S_{T,3}) = \{S'_2, S'_5\}, OUT(S'_{T,3}) = S'_1; IN(S_{T,4}) = S'_3, OUT(S_{T,4}) = S'_4 \\ IN(S_{T,5}) = S'_4, OUT(S_{T,5}) = S'_3; ...; IN(S_{T,7}) = S'_5, OUT(S_{T,7}) = S'_6 \\ IN(S_{T,8}) = S'_6, OUT(S_{T,8}) = S'_{END} \\ \{S'_0\} \\ \{S'_{END}\} \end{cases} \quad (11)$$

In equation (11), S'_0 to S'_{END} represents the initial motion state, a certain position on the field, a distance between the soccer ball and the robot exceeding 500mm, a distance less than 500mm, a suitable shooting position, a shooting position, a shooting position, and an ending state. $S_{T,0}$ - OUT corresponds to the starting stage, the stage where the ball is detected and the distance between the ball and the robot exceeds 500mm, the stage where the ball is detected but the distance is less than 500mm, the stage where the ball is not detected, the stage where the target is detected, the stage where the target is no longer detected, the stage where the offset is within the allowable range and in the correct shooting position, the stage where the absolute angle deviation between the robot and the target is less than 2°, and the end stage. The ideal shooting position can be obtained through the above calculation, but the action during task execution may cause deviation in joint volume, so it is necessary to correct the shooting position. SR kicking display in different directions, as shown in Figure 7.

In Figure 7, a Petri net for the forward is constructed. SI is the ideal shooting position. Simultaneously constructing a coordinate system centered around the soccer for subsequent analysis, the expression for the relative coordinate offset can be obtained, as shown in equation (12).

$$\begin{cases} \Delta x = r_F + d' + d_{A-T} \\ \Delta y = y_b - y_r \end{cases} \quad (12)$$

In equation (12), Δx and Δy are the offsets along the X-axis and Y-axis directions. r_F, d', and d_{A-T} correspond to the soccer radius, the reserved distance to avoid accidental contact, and the horizontal distance between the ankle joint and toes. y_b and y_r are the centroid positions of SR's body and right lower limb. Then, by converting to an absolute coordinate system, the absolute coordinates of the shooting position can be obtained, as shown in equation (13).

$$\begin{cases} x_{robert} = x_F - \Delta x \cos(\theta_2 - \theta_1) + \Delta y \sin(\theta_2 - \theta_1) \\ y_{robert} = y_F - \Delta x \sin(\theta_2 - \theta_1) - \Delta y \cos(\theta_2 - \theta_1) \end{cases} \quad (13)$$

In equation (13), x_{robert} and y_{robert} are the horizontal and vertical coordinates of the robot's shooting position in the absolute coordinate system. Overall, the design of SR control strategy can be completed.

3 Results

To test the feasibility of the research method, this study first analyzes the effectiveness of the improved YOLO v5 target recognition method and the path planning method that integrates the RRT algorithm as the basic methods. Then, a comprehensive analysis is conducted

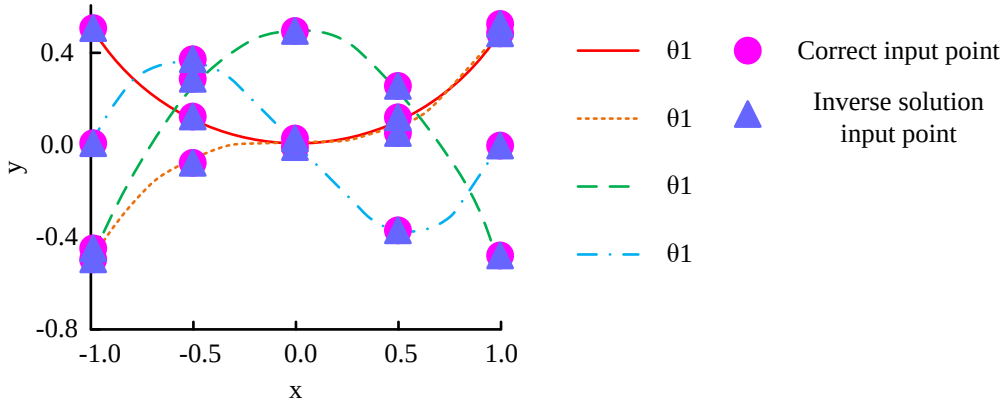

Figure 8: Results of inverse kinematics solution.

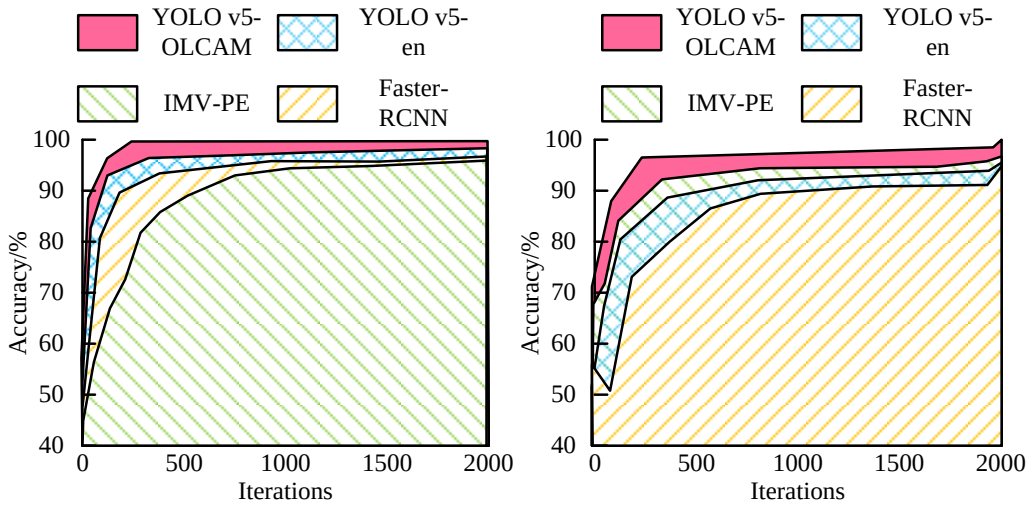

(a) Accuracy results for size 1 (b) Accuracy results for size 2

Figure 9: The results of different target recognition methods at various input image sizes.

on the SR control strategy that integrates the RRT algorithm.

3.1 Performance analysis of target recognition method based on improved YOLOv5

To investigate the performance of the YOLO v5-OLCAM, the experimental environment is selected to test the software Matlab R2024b, and the trained method is translated into C++code. The experimental environment is set as follows: the CPU is selected as Intel Core i7-9700K @ 3.60GHz, the GPU is NVIDIA GeForce RTX 2080 Ti, and the memory is 512GB NVMe SSD. The Ball Detection Dataset (BDD) specifically designed for the Robot Soccer Standard Platform League is selected as the testing dataset. It is mainly used for training and evaluating ball detection algorithms. This dataset contains 1,000 images of different resolutions. All images contain detailed bounding box annotations indicating the position and size of the ball. In addition, to improve the generalization ability of the model, data augmentation techniques are applied during the training process. Finally, images under different lighting conditions (such as daylight, cloudy, indoor lighting) and different site environments (such as grassland, artificial turf) are included, providing rich training samples for the model. In addition, the dataset includes a 70% training set and 15% validation and testing sets. The experimental parameters of YOLO v5-OLCAM are set as follows: the initial learning rate and maximum iteration times are 0.001 and 2000, and the amount of data processed in one batch is 32. Two image sizes, 20*20*1 (size 1) and 128*128*3 (size 2), are used for testing. Among them, $128\times128\times3$ are conventional sizes that meet the visual input requirements of SRs. $20\times20\times1$ is a very small size, only used to verify the robustness of the research model under resource constraints. In addition, by comparing the target detection performance under different sizes, the accuracy and robustness of the model can be more comprehensively evaluated. To more scientifically validate the performance

of research methods, advanced methods such as YOLO v5-en, Integrated Machine Vision and Proximity Estimation (IMV-PE), and Faster Region-based Convolutional Neural Networks (Faster-RCNN) are compared. Meanwhile, this study uses two

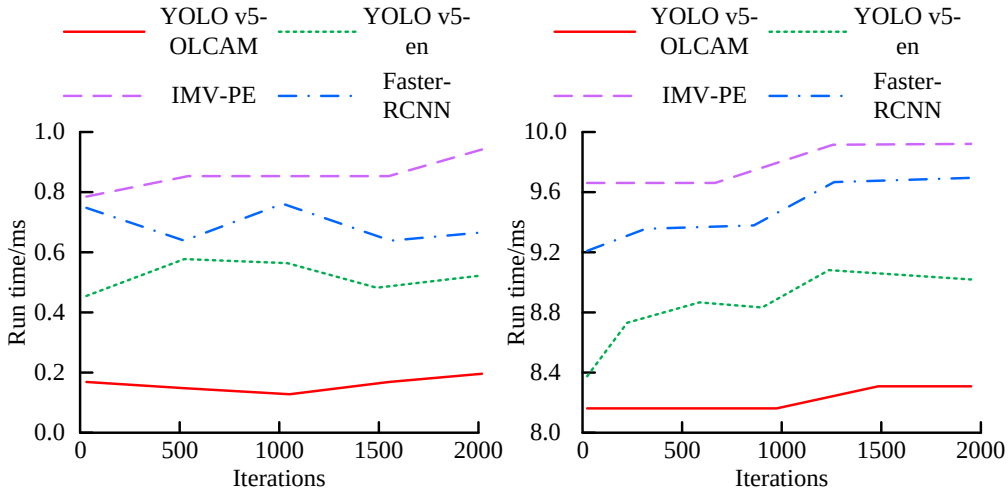

(a) Running time results under size 1 (b) Running time results under size 2

Figure 10: Comparison of computational efficiency results of different target recognition methods.

Table 2: Performance of research methods in different datasets.

Data set	Accuracy/%	Recall rate/%	F1 value	AUC
Training set	99.35	99.28	0.9931	0.9992
Validation set	99.12	98.97	0.9904	0.9987
Test set	99.07	98.83	0.9895	0.9983

commonly used indicators, accuracy and runtime, to evaluate the effectiveness of each method. The evaluation indicators are calculated by taking the mean and variance of 20 experiments and setting a 95% confidence interval. The study first validates the kinematic modeling of the NAO robot and obtains the inverse kinematics solution results, as shown in Figure 8.

Figure 8 shows that the inverse solution of the robot can further obtain the corresponding joint angles. Figure 9 shows the accuracy results of different target recognition methods.

Figures 9 (a) and (b) show the accuracy of four methods for size 1 and size 2. In very small image sizes, YOLO v5-OLCAM and YOLO v5-en, which have undergone lightweight processing, both achieve high accuracy, reaching 99.12% and 97.56% when stable. In conventional image sizes, the research method can still demonstrate excellent accuracy, reaching 99.07%. The Faster-RCNN method has the worst performance, but different object recognition methods can maintain an accuracy of over 87% after reaching stability. The above results may be due to the lower background complexity of size 1 images in the BDD dataset, which has higher annotation quality and is beneficial for the model to better learn target features during training. At the same time, the research method utilizes the channel attention and spatial attention mechanisms of the LCAM module, which can more effectively extract key features of small-sized images. The computational efficiency comparison of different target recognition methods is shown in Figure 10.

Figures 10 (a) and (b) show the calculation results of each method for dimensions 1 and 2. Under different image sizes, the YOLO v5-OLCAM method exhibits high computational efficiency, especially in small-sized images. This is because it introduces LCAM for optimization and improves the feature extraction process without adding too much computational burden. The research method has an average running time of 0.19ms and 8.2ms for sizes 1 and 2. The computational efficiency performance of YOLO v5-en is second, as this method has also undergone some lightweight design, but it cannot handle more complex images. To further investigate the performance changes of research methods on the training set, validation set, and test set, the accuracy, recall rate, F1 value, and Area Under the Curve (AUC) are studied. The results are shown in Table 2.

According to Table 2, the accuracy of the test set decreased by 0.28% compared to the training set, indicating that the research method has excellent generalization ability. Moreover, the recall rate of the research method exceeded 98% in all subsets, and the AUC values also exceeded 0.998, indicating its stability and robustness. To investigate the effectiveness of each module of the research method, ablation experiments were conducted, and the results are shown in Table 3.

Table 3 shows that the recall rate of the method combined with the LCAM module increased by 6.2%, and the recall rate of the method improved by multi-scale fusion increased by 9.5%. The optimal recall rate of the complete method was 94.6%, and the inference time was 3ms, which still met real-time requirements. The above results were due to the fact that LCAM improved recognition performance with minimal computational cost, while the complete method achieved optimal balance

through the synergistic effect of LCAM and multi-scale fusion optimization.

Table 3: Results of ablation experiment.

Method	Inference time/ms	Parameter quantity/M	FPS	Recall rate/%
Baseline model	2.4	7.2	416	82.7
Baseline model+LCAM	2.6	7.3	385	88.9
Baseline model+multi-scale fusion improvement	2.9	7.5	345	92.2
YOLO v5-OLCAM	3.0	7.6	313	94.6

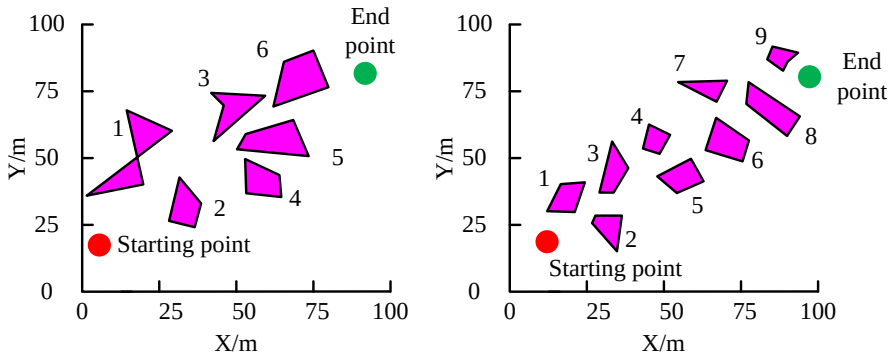

(a) Map A (b) Map B

Figure 11: Experimental map schematic diagram.

Table 4: Comparison results of indicators for various methods.

Experimental Map	Path planning method	Number of iterations	Length/cm	Nodes	p-value
A	Improved RRT-PRM	800	19.637 ± 0.42*	717	/
	DRL-LDS	1600	22.642 ± 0.58	1325	<0.001
	IRRT-DTGS	2300	27.265 ± 0.76	2167	<0.001
	IDDQN	3000	30.084 ± 0.91	2793	<0.001
B	Improved RRT-PRM	1700	26.713 ± 0.51	1375	/
	DRL-LDS	2200	29.165 ± 0.63	1963	0.002
	IRRT-DTGS	3500	34.265 ± 0.85	2647	<0.001
	IDDQN	4000	37.652 ± 1.12	3266	<0.001

3.2 Performance analysis of path planning method integrating RRT algorithm

To test the performance of the proposed path planning method, this study conducted experiments using the SimRobot platform, specifically designed for robot simulation, to simulate various complex scenarios. It also introduced existing mainstream path planning methods for comparative experiments, including Deep Reinforcement Learning Combined with Large-scale Domain Search (DRL-LDS), Improved RRT Based on Dual Tree Growth Strategy (IRRT-DTGS), and Improved Deep Double Q-Network (IDDQN). To analyze the adaptability of different path planning methods, this study conducted multiple experiments on different maps. The specific experimental maps are shown in Figure 11.

Figures 11 (a) and (b) show the experimental maps A and B. There are 6 and 9 obstacles on the two maps. The above two types of maps are both represented by vector maps and obstacles are represented by polygons. Each obstacle is conveniently measured and updated accurately through robot sensor data. During the path planning process, the vector map is updated in real-time to reflect changes in the collision detection environment. Table 4 compares the performance of different methods.

In Table 4, in Map A, the improved RRT-PRM only needs 800 iterations to plan a path length of 19.637cm, and 717 nodes are used. This indicates that the research method has high efficiency and short path planning ability, while IDDQN performs the worst, requiring 3,000 iterations to obtain a planned path length of 30.084cm. In Map B, the research method requires 1,700 iterations to obtain a planned path of 26.713cm. This indicates that the research method maintains superiority in terms of iteration times and path length, and has significant statistical significance compared to other methods ($p<0.001$). To further explore the performance effect of research methods in competition scenarios, this study conducts experiments through a simulation platform. The opposing robot is set as an obstacle and its position is random.

During this process, the search step size and the probability of determining random sampling points are set to 5cm and 0.5. The random competition scenario simulates the dynamic environment of robot soccer matches, and the opponent's movements are modeled using conventional obstacle avoidance

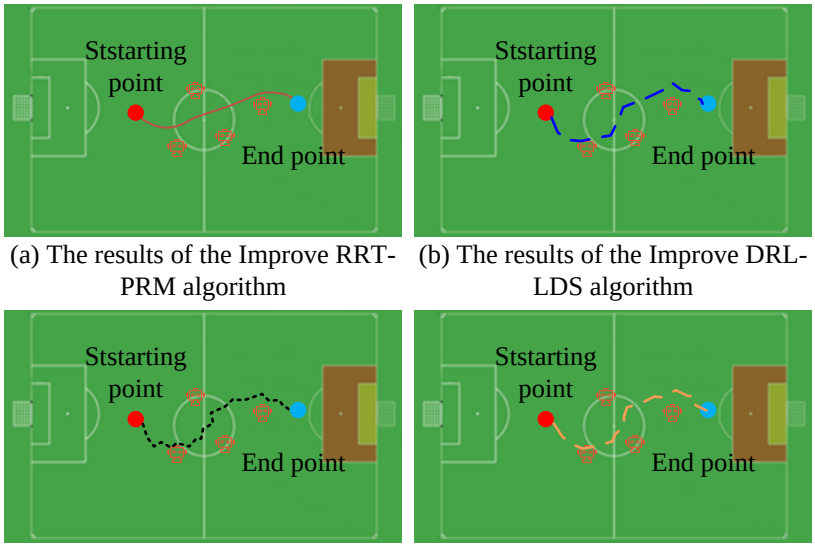

(a) The results of the Improve RRT-PRM algorithm

(b) The results of the Improve DRL-LDS algorithm

(c) The results of the IRRT-DTGS algorithm

(d) The results of the IDDQN algorithm

Figure 12: Simulation results of different path planning algorithms in random competition scenarios.

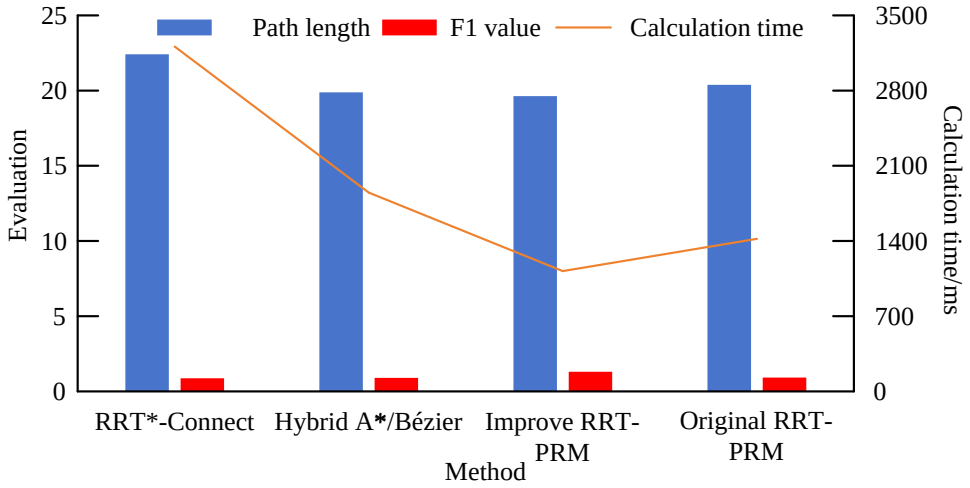

Figure 13: Results of ablation experiment.

Table 5: Bézier performs curvature results.

Stage	Maximum curvature	Curvature variance
Before smoothing	12.7	6.34
After smoothing	4.2	1.07

algorithms. The simulation comparison of various algorithms is shown in Figure 12.

Figures 12 (a)-(d) correspond to the simulation effects of improved RRT-PRM, DRL-LDS, IRRT-DTGS, and IDDQN in a random competition scenario. The path planned by the research method can effectively avoid the opponent robot, and the path distance is short. The position of the turning point also has a small curvature, which meets the path planning requirements of SR in actual competition. The planning path length of other methods is relatively longer and there are many turning points, so the performance of path planning is relatively poor. In addition, the study introduces RRT*-Connect, Hybrid A*/Bézier, and the original RRT-PRM method for comparative experiments, and conducts ablation experiments on the research method. The results are shown in Figure 13.

As shown in Figure 13, the path of the research method is 19.63cm, indicating that the local optimization ability of PRM can eliminate redundant nodes on the RRT coarse path. The longest path of RRT*-Connect is 22.41cm, and its performance is the worst. The F1 value

of the original RRT-PRM is 0.921, while the F1 value of the improved RRT-PRM is 0.983, indicating a significant improvement in the quality of the improved path. A quantitative analysis of curvature is conducted on Bézier, and the comparison before and after smoothing is shown in Table 5.

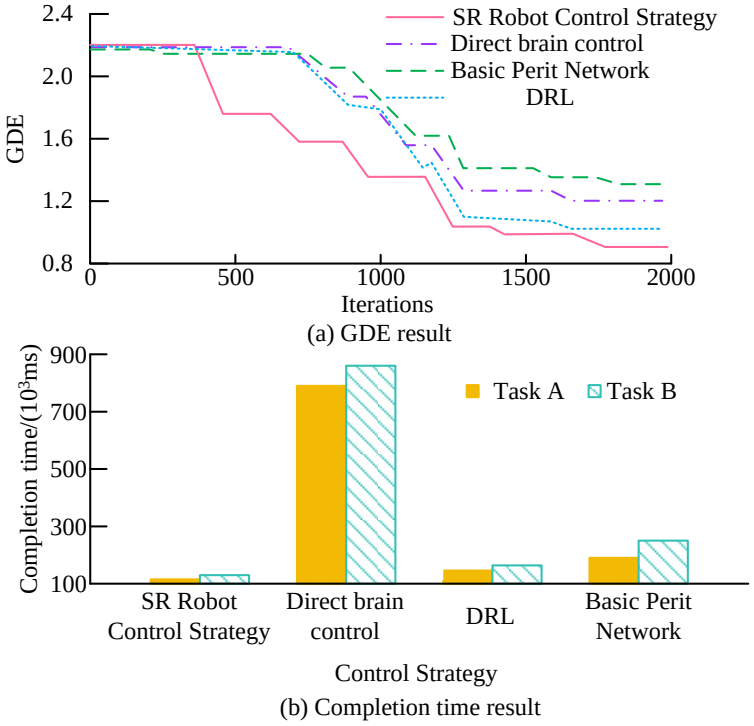

Figure 14: Simulation results of different path planning algorithms in random competition scenarios.

Table 5 shows that Bézier processing can effectively reduce the maximum curvature and curvature variance, and the smoothing effect is significant.

3.3 Analysis of SR control strategy results integrating RRT algorithm

To verify the performance and application effectiveness of SR control decision-making by integrating the RRT algorithm and Petri net, this study first sets two tasks. Task A requires SR to sequentially reach designated obstacles 1, 3, and 6 on map A. Task B requires SR to sequentially reach obstacles 2, 5, and 8 on map B. To verify the SR control strategy more scientifically, a comparative experiment is conducted using Deep Reinforcement Learning (DRL), Direct Brain Control, and Basic Perit Network control strategies. The performance is evaluated using completion time and Global Decision Entropy (GDE).The direct brain control strategy is a method in which robots use the EEG signals generated by human brain activity to manipulate external devices. The completion time and GDE can reflect the performance of control strategies in practical applications from different perspectives, and are the most relevant indicators for evaluating the effectiveness of SR control strategies. The completion time can directly reflect the efficiency of task execution, and it is not only related to the efficiency of path planning but also closely related to the stability of motion control. Therefore, it can comprehensively reflect the synergistic effect of path planning and motion control. GDE measures the degree of uncertainty in the decision-making process and reflects the adaptability and stability of the control strategy in complex environments. Figure 14 shows the performance comparison of different control strategies.

Figures 14 (a) and (b) correspond to GDE and completion time for different control strategies. When the control strategy is iterated to 2,000 times, the GDE values of SR control strategy, direct brain control strategy, and basic Perit network control strategy are 0.934, 1.175, and 1.386, respectively. This indicates that the research method has less uncertainty in the decision-making process, and it has more information to make decisions, which in turn makes the decision results more accurate and reliable. The performance of the DRL method is relatively high, with an entropy fluctuation range of ± 0.15, indicating a problem with strategy stability. In addition, the research method has the shortest task completion time for task A and task B, which are 115,000ms and 130,000s, respectively. The above successful attempts demonstrate that the robot can smoothly reach the designated position and complete the task in the given task, which directly reflects the effectiveness and feasibility of the control strategy in practical tasks. However, the direct brain control strategy shows multiple dead loops, while the research method only shows one dead loop, indicating that it performs better in terms of stability. The comparison of different control strategies in the competition scenario is shown in Figure 15.

Figure 15 (a) shows the results of various control strategies in the game scenario, and Figure 15 (b) shows the scene of shooting using the research method. The SR control strategy falls into a dead loop once and succeeds 48 times in the competition scenario, with an average

planning time of only 26.8 seconds. The number of times the direct brain control falls into a dead loop corresponds to 6 and 42 successful cycles, with the longest average planning time of 36.2 seconds. The above successful attempts have confirmed the ability of the research

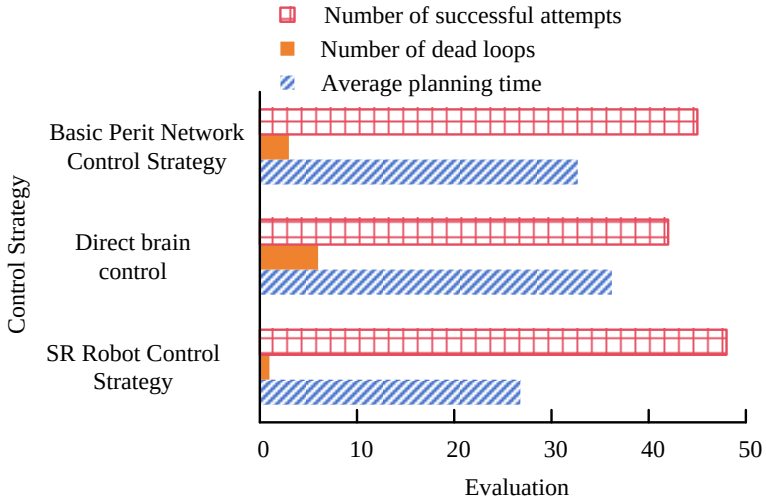

(a) The results of different control strategies in competition scenarios

(b) Schematic diagram of shooting scene using research methods

Figure 15: The results of different control strategies in competition scenarios.

method to complete tasks in dynamic, complex, and highly competitive environments, which to some extent reflects the adaptability and robustness of the research method in practical competitive scenarios. This indicates that the research method can effectively respond to unexpected situations and can be applied in a wider range of scenarios.

4 Discussion

With the progress of AI technology, motion control, and sensors, robots are no longer limited to industrial production lines and service areas, but have entered competitive sports. Especially in high-demand sports such as soccer, it demonstrates its strong potential and future prospects. Therefore, this study first constructed an SR kinematic analysis method and optimized the target recognition part, proposing the YOLO v5-OLCAM algorithm. Then, an improved RRT-PRM algorithm was designed for the path planning part. Finally, based on the above methods, an SR control strategy integrating the RRT algorithm and Petri was proposed.

Research has shown that compared to methods such as YOLO v5-en, IMV-PE, and Faster-RCNN, the YOLO v5-OLCAM method exhibited higher accuracy and lower runtime at different image sizes. This indicated that introducing LCAM could significantly optimize the efficiency and accuracy of feature extraction without increasing excessive computational burden. In small-sized images, the runtime of YOLO v5-OLCAM was only 0.19ms, while YOLO v5-en was 0.5ms, making this method more suitable for real-time operation on resource-constrained robot platforms. The above results may be due to the introduction of LCAM and the improvement of multi-scale feature network fusion, as well as the use of data augmentation techniques in the training process to enhance the generalization ability of the research method. The improved RRT-PRM method outperformed mainstream methods such as DRL-LDS, IRRT-DTGS, and IDDQN in terms of path planning efficiency and smoothness in complex map scenes. This is mainly due to the combination of the fast exploration ability of the RRT algorithm and the efficient query ability of the PRM method, as well as the smoothing processing of the path by the Bezier curve. Specifically, in Map A, the improved RRT-PRM method only required 800 iterations to plan a path of 19.637cm, while IDDQN required 3,000 iterations to obtain a path of 30.084cm. This indicated that the improved RRT-PRM method had significant advantages in terms of efficiency and path quality in path planning. Finally, the control strategy incorporating the RRT algorithm outperformed both direct brain control and basic Petri net control strategies in terms of GDE and average planning time. This indicated that through Petri net role modeling and motion state analysis, uncertainty in the

decision-making process could be effectively reduced, and the accuracy and reliability of decision-making could be improved. In tasks A and B, the completion time of the research method was 115 seconds and 130 seconds, while the average planning time for direct brain control was the longest, requiring 36.2 seconds. This indicated that the control strategy incorporating the RRT algorithm had higher efficiency and stability in complex competition scenarios.

Compared with the advanced method of related worksheets, the research method can still maintain high accuracy at extremely low resolutions. The improved dragonfly optimization algorithm based on the fusion of Q-learning and the dynamic window method in reference [12] has excellent computational efficiency, but its performance will significantly decrease in low-resolution images. This may be due to its inability to handle complex scenes. The improved RRT-PRM method performs well in dynamic competition scenarios, effectively avoiding dynamic obstacles and planning smooth and efficient paths. In contrast, the improved dragonfly optimization algorithm based on the fusion of Q-learning and the dynamic window method performs poorly in dynamic environments, with poor path smoothness and multiple iterations. The above results may be due to the research method combining the fast exploration ability of the RRT algorithm and the efficient query ability of the PRM method, and smoothing the path through a Bezier curve to ensure that the path conforms to the kinematic constraints of the robot.

In summary, the contribution and novelty of the LCAM module were confirmed in the ablation experiment of YOLOv5-OLCAM, with a recall rate increase of 6.2%. In terms of path planning, the improved RRT-PRM method reduced path redundancy by 32.5% compared to the traditional RRT* algorithm. By introducing third-order Bezier curve smoothing, the path curvature variance was reduced from 6.34 to 1.07, significantly better than the curvature variance of 3.82 in reference [13]. The proposed target recognition method still has room for improvement, and in future research, more advanced and lightweight multi-scale feature fusion methods can be used to improve computational efficiency while ensuring recognition accuracy.

5 Conclusion

This study focused on SR and first conducted kinematic analysis. Then, YOLO v5-OLCAM algorithm was designed for the target recognition part, and an improved RRT-PRM was proposed for SR path planning. Finally, an SR control strategy that integrates RRT algorithm and Petri was established. In the experiment, among the comparison of different object recognition methods, YOLO v5-OLCAM performed the best in different image sizes, with the highest accuracy of 99.12% and the lowest running time of 0.19ms. The accuracy of other mainstream target recognition methods exceeded 87%, and the YOLO v5-en method had relatively good computational efficiency, with a running time of 0.5ms in size 1. In the comparison of different path planning methods, the improved RRT-PRM method only needed 1,700 iterations to obtain the shortest planned path in complex map scenes, which was 26.713cm. Its planned path had good smoothness, which was very suitable for the operation rules of robots. Finally, in the comparison of different control strategies, the GDE value of the research method was only 0.934, indicating that its decision results were more reliable, and it had the least number of dead loops, only once, with the shortest average planning time of 26.8 seconds. In summary, the research method could achieve smoother path planning and more stable action performance, as well as precise target recognition, which is beneficial for improving SR's performance in soccer matches.

Fundings

The research is supported by: China Social Science Foundation's "Thirteenth Five Year Plan" 2020 Education General Project (No. BLA200218).

References

[1] Menglin Wu, and Zhenyu Liu. Unmanned logistics vehicle control based on path tracking control algorithm. Informatica, 48(2):239-253, 2024. https://doi.org/10.31449/inf.v48i2.5940

[2] A. Teklu, and J. Mozaryn. Trajectory tracking control of robot manipulator using hybrid control strategy. Acta Physica Polonica A, 146(4):430-437, 2024. https://doi.org/10.12693/APhysPolA.146.430

[3] Muhammad Shakaib Iqbal, Hazrat Ali, Son N. Tran, and Talha Iqbal. Coconut trees detection and segmentation in aerial imagery using mask region-based convolution neural network. The Institution of Engineering and Technology, 21(5):428-439, 2021. https://doi.org/10.1049/cvi2.12028

[4] Yu-Teng Chang, and Neng-Hsun Fan. A novel approach to market segmentation selection using artificial intelligence techniques. The Journal of Supercomputing, 79(12):1235-1262, 2023. https://doi.org/10.1007/s11227-022-04666-2

[5] Peng Wei, Shilian Wang, Junshan Luo, Yan Liu, and Li Hu. Optimal frequency-hopping anti-jamming strategy based on multi-step prediction Markov decision process. Wireless Networks, 27(7):4581-4601, 2021. https://doi.org/10.1007/s11276-021-02735-7

[6] E. W. Andarge, A. Ordys, and Y. M. Abebe. Mobile robot navigation system using reinforcement learning with path planning algorithm. Acta Physica Polonica A, 146(4):452-456, 2024. https://doi.org/10.12693/APhysPolA.146.452

[7] Hussain K. Chaiel, and Ahmed A. Alabdel Abass. Game theoretical model for information transmission in structure-free wireless sensor networks. The Institution of Engineering and Technology, 20(17):3080-3086, 2020. https://doi.org/10.1049/iet-com.2019.1216

[8] Xuanang Chen, and Peijun Gao. Path planning and control of soccer robot based on genetic algorithm.

Journal of Ambient Intelligence and Humanized Computing, 11(12):6177-6186, 2020. https://doi.org/10.1007/s12652-019-01635-1

[9] Yuheng Zhang, Yizhun Peng, Lianchen Zhao, Zhou Zhang, and Wanlong Peng. Design of an embedded humanoid soccer robot based on image processing. Journal of Advances in Artificial Life Robotics, 1(2):76-80, 2020. https://doi.org/10.57417/jaalr.1.2_76

[10] Alexandre F. V. Muzio, Marcos R. O. A. Maximo, and Takashi Yoneyama. Deep reinforcement learning for humanoid robot behaviors. Journal of Intelligent & Robotic Systems, 105(1):12-27, 2022. https://doi.org/10.1007/s10846-022-01619-y

[11] Xingli Gan, Zhihui Huo, and Wei Li. DP-A*: For path planning of UGV and contactless delivery. IEEE Transactions on Intelligent Transportation Systems, 25(1):907-919, 2024. https://doi.org/10.1109/TITS.2023.3258186

[12] Awei Zou, Lei Wang, Weimin Li, Jingcao Cai, Hai Wang, and Tielong Tan. Mobile robot path planning using improved mayfly optimization algorithm and dynamic window approach. The Journal of Supercomputing, 79(8):8340-8367, 2023. https://doi.org/10.1007/s11227-022-04998-z

[13] Gang Hu, Bo Du, and Guo Wei. HG-SMA: Hierarchical guided slime mould algorithm for smooth path planning. Artificial Intelligence Review, 56(9):9267-9327, 2023. https://doi.org/10.1007/s10462-023-10398-3

[14] Steve Macenski, Shrijit Singh, Francisco Martín, and Jonatan Ginés. Regulated pure pursuit for robot path tracking. Autonomous Robots, 47(6):685-694, 2023. https://doi.org/10.1007/s10514-023-10097-6

[15] Shiliang Shao, Jin Zhang, Ting Wang, Achyut Shankar, and Carsten Maple. Dynamic obstacle-avoidance algorithm for multi-robot flocking based on improved artificial potential field. IEEE Transactions on Consumer Electronics, 70(1):4388-4399, 2024. https://doi.org/10.1109/TCE.2023.3340327

[16] Jun Sugawara, Nana Ogoh, Hironobu Watanabe, Shotaro Saito, Maki Ohsuga, Tetsuya Hasegawa, Narumi Kunimatsu, and Shigehiko Ogoh. Attenuated arterial wave reflection associated with fatigue in youth women's football tournament: Impact of match-repetition. Medicine & Science in Sports & Exercise, 56(10S):42-42, 2024. https://doi.org/10.1249/01.mss.0001052856.41034.bf

[17] David Brinkjans, Yannik Paul, Jürgen Perl, and Daniel Memmert. The success-score in professional football: A metric of playing style or a metric of match outcome? International Journal of Computer Science in Sport, 23(1)54-79, 2024. https://doi.org/10.2478/ijcss-2024-0004

[18] Zhaoliang Sheng, and Shengyuan Xu. An aperiodic-sampling-dependent event-triggered control strategy for interval type-2 fuzzy systems: new communication scheme and discontinuous functional. IEEE Transactions on Cybernetics, 54(11):6436-6447, 2024. https://doi.org/10.1109/TCYB.2024.3432909

[19] Binyamin Yusoff, Dian Pratama, Adem Kilicman, and Lazim Abdullah. Circular intuitionistic fuzzy ELECTRE III model for group decision analysis. Informatica, 34(4):881-908, 2023. https://doi.org/10.15388/23-INFOR536

[20] Francesco Della Villa, Bruno Massa, Antonio Bortolami, Gianni Nanni, Jesus Olmo, and Matthew Buckthorpe. Injury mechanisms and situational patterns of severe lower limb muscle injuries in male professional football (soccer) players: A systematic video analysis study on 103 cases. British Journal of Sports Medicine, 57(24):1550-1558, 2023. https://doi.org/10.1136/bjsports-2023-106850

[21] Giovanni Ercolano, Silvia Rossi, Daniela Conti, and Alessandro Di Nuovo. Gesture recognition with a 2D low-resolution embedded camera to minimize intrusion in robot-led training of children with autism spectrum disorder. Applied Intelligence, 54(8):6579-6591, 2024. https://doi.org/10.1007/s10489-024-05477-z

[22] Alvaro Paz, and Gustavo Arechavaleta. Analytical differentiation of the articulated-body algorithm: A geometric multilinear approach. Multibody System Dynamics, 53(3):347-373, 2023. https://doi.org/10.1007/s11044-023-09907-7

[23] Tasuku Furube, Masashi Takeuchi, Hirofumi Kawakubo, Kazuhiro Noma, Naoaki Maeda, Hiroyuki Daiko, Koshiro Ishiyama, Koji Otsuka, Yoshihito Sato, Kazuo Koyanagi, Kohei Tajima, Rodrigo Nicida Garcia, Yusuke Maeda, Satoru Matsuda, and Yuko Kitagawa. ASO visual abstract: Usefulness of an artificial intelligence model in recognizing recurrent laryngeal nerves during robot-assisted minimally invasive esophagectomy. Annals of Surgical Oncology, 31(13):9364-9365, 2024. https://doi.org/10.1245/s10434-024-16269-7

[24] Qinggang Wu, Yang Li, Wei Huang, Qiqiang Chen, and Yonglei Wu. C3TB-YOLOv5: Integrated YOLOv5 with transformer for object detection in high-resolution remote sensing images. International Journal of Remote Sensing, 45(7/8):2622-2650, 2024. https://doi.org/10.1080/01431161.2024,2329528

[25] J. Jayachitra, K. S. Devi, M. S. K. Satti, and Satish Kumar Satti. Terahertz video-based hidden object detection using YOLOv5m and mutation-enabled salp swarm algorithm for enhanced accuracy and faster recognition. The Journal of Supercomputing, 80(6):8357-8382, 2024. https://doi.org/10.1007/s11227-023-05717-y

[26] Mervenur Çakır, Murat Ekinci, Elif Baykal Kablan, and Mürsel Şahin. AVD-YOLOv5: A new lightweight network architecture for high-speed aortic valve detection from a new and large echocardiography dataset. Medical & Biological Engineering & Computing, 62(8)2511-2528, 2024. https://doi.org/10.1007/s11517-024-03090-3

[27] Kaisi Yang, Lianyu Zhao, and Chenglin Wang. Workpiece tracking based on improved SiamFC++

and virtual dataset. Multimedia Systems, 29(6):3639-3653, 2023. https://doi.org/10.1007/s00530-023-01185-9

[28] Zhiqing Wen, Yi He, Sheng Yao, Wang Yang, and Lifeng Zhang. A self-attention multi-scale convolutional neural network method for SAR image despeckling. International Journal of Remote Sensing, 44(12):902-923, 2023. https://doi.org/10.1080/01431161.2023,2173029

[29] Duona Zhang, Yuanyao Lu, Yundong Li, Wenrui Ding, and Baochang Zhang. High-order convolutional attention networks for automatic modulation classification in communication. IEEE Transactions on Wireless Communications, 22(7):4600-4610, 2023. https://doi.org/10.1109/TWC.2022,3227518

[30] Kavita Bhosle, and Vijaya Musande. Evaluation of deep learning CNN model for recognition of devanagari digit. Artificial Intelligence and Applications, 1(2):114-118, 2023. https://doi.org/10.47852/bonviewAIA3202441

[31] Gangadhar Bandewad, Kunal P. Datta, Bharti W. Gawali, and Sunil N. Pawar. Review on discrimination of hazardous gases by smart sensing technology. Artificial Intelligence and Applications, 1(2):86-97, 2023. https://doi.org/10.47852/bonviewAIA3202434